Astron. Astrophys. 325, 839–846 (1997)

ASTRONOMY AND ASTROPHYSICS

# Ion emission line profiles in cometary plasma tails

**H. Rauer**[1], **F. Roesler**[2], **F. Scherb**[2], **H.U. Schmidt**[3], **and R. Wegmann**[3]

[1] Observatoire de Paris-Meudon, 5, Place Jules Janssen, F-92195 Meudon Cedex, France
[2] University of Wisconsin, Madison, Wisconsin 53706, USA
[3] MPI für Astrophysik, D-85748 Garching, Germany

Received 13 December 1996 / Accepted 2 April 1997

**Abstract.** We present a first attempt to model the profile of ion emission lines in a cometary plasma tail with the aid of a 3D-MHD model of the comet-solar wind interaction, and to compare the calculated line profiles to high-resolution measurements of the $H_2O^+$ doublet at 6159 Å in comet 1P/Halley on January 6, 1986. The modelled line profiles are asymmetric and show a high velocity wing originating from fast ions in the outer parts of the tail along the line-of-sight. Comparison with the measured profiles shows that such high-velocity wings are indeed observed and are needed to fully approximate the observed profiles.

We performed a quantitative analysis of the contribution of fast ions to the ion flow to examine if they are really sufficient to explain the discrepancy between measured $H_2O^+$ production rates and the rates expected from photoionization of water. It is found that the combined effect of fast ions and the limited field-of-view can indeed reduce the measured flux. However, the reduction seems not be sufficient to explain the whole discrepancy.

**Key words:** comets: general – comets: 1P/Halley

## 1. Introduction

Analysing the profiles of emission lines of cometary ions can reveal information on their density and velocity distribution in the plasma tail along the line-of-sight, LOS. However, the ion distribution in the cometary tail is determined by the interaction of the comet with the solar wind and sophisticated models of this process are needed to interpret the observed profiles. The basic asymmetric shape to be expected in ion emission lines emitted in the tail was pointed out (Rauer et al., 1995) with the help of a 3-D MHD model (Schmidt-Voigt 1989) of the comet-solar wind interaction. In this paper we use the ion distribution derived from the model to calculate the profiles of $H_2O^+$ emission lines. The resulting lines are then compared to high-resolution spectra of the $H_2O^+$ doublet at 6159 Å observed in comet 1P/Halley in January 1986 (Scherb et al., 1990).

$H_2O^+$ production rates measured from the ground are much lower than the values expected from the ionisation of water. This discrepancy was explained by the assumption that emission of ions far from the tail axis is too faint to be detected, but yet could contribute significantly to the ion flux (DiSanti et al., 1990; Rauer & Jockers 1993; Scherb et al. 1990; Schultz et al., 1993). This interpretation was first put forward by McComas et al. (1987) from measurements of the electron density by the ICE spacecraft in the tail of comet Giacobini-Zinner, assuming that only ions in the dense current sheet would be seen in ground-based observations. Analysis of ion emission lines derived from a model of the cometary plasma tail and the comparison with measurements allows to test this assumption.

*Send offprint requests to*: H. Rauer

**Table 1.** Comet and solar wind parameters used in the model.

| **comet** | | **solar wind** | |
|---|---|---|---|
| gas production rate | $10^{29}$ s$^{-1}$ | mass density | 5 m$_p$ cm$^{-3}$ |
| velocity of neutrals | 1 km s$^{-1}$ | velocity | 400 km s$^{-1}$ |
| ionisation rate | $10^{-6}$ s$^{-1}$ | temperature | 5 $10^4$ K |
| mean molecular weight | 20 m$_p$ | magnetic field | 5 nT |

## 2. The model

The 3-D MHD model used is described in Schmidt-Voigt (1989) and Rauer et al. (1995). The model is designed to study large scale phenomena in cometary ion tails. The model box extends 3 $10^5$ km towards the sun and to either side of the nucleus. It covers 7 $10^5$ km in the tail direction. The model box is divided by nonequidistant grid points into $28\times28\times46$ cells with a minimal resolution of $\approx$8000 km around the nucleus. This seems to be sufficient to represent the gross features of a cometary plasma tail as they are seen in low spatial resolution ground-based measurements. Table 1 shows the comet and solar wind parameters used in the model run (see Rauer et al., 1995).

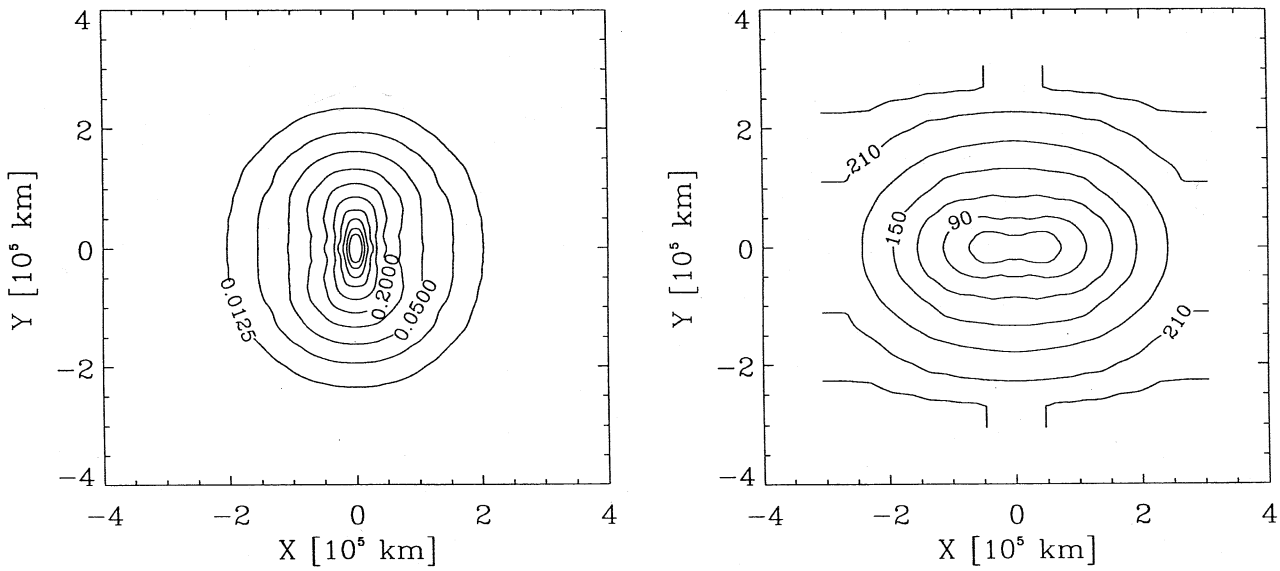


**Fig. 1a and b.** Cut perpendicular to the tail axis, 4 $10^5$ km behind the nucleus. **a** ion number density [$cm^{-3}$]; **b** velocity along tail axis [km $s^{-1}$].

For simplicity, the interplanetary magnetic field (IMF)in the unperturbed solar wind is assumed perpendicular to the solar wind velocity in the rest frame of the comet. We expect deviations from this assumption to have only minor effects on the line profiles integrated along the LOS. We therefore choose the IMF parallel to the x-axis, and the solar wind to stream along the z-axis. We can define two perpendicular planes: the plane containing the magnetic field: the xz-, or IMF, plane, and the perpendicular yz-, or equatorial, plane.

The variability in cometary plasma tails introduced by, for example, changes in the onstreaming solar wind makes the detailed comparison of models with observations difficult. The solar wind parameters at a comet are generally not known for the time of ground-based observations. Because of the resulting uncertainties, we use stationary conditions for the model and assume that they represent the mean conditions during the observing time.

The major characteristics of stationary plasma tails are described in numerous places. Here, we only summarize briefly the major features needed to understand the derived emission line profiles and resulting conclusions. Due to the interplanetary magnetic field draping around the comet, the ions are compressed in a flat sheet in the equatorial plane by magnetic curvature and pressure forces (see Fig. 1a and b). This leads to a bright, narrow appearance of the ion tail when looking onto the IMF-plane and a fainter, wider appearance when viewing the perpendicular side (equatorial plane). Because the magnetic forces can accelerate the flow only perpendicular to the draped field lines, the ions move in the equatorial plane, i.e. the center plane of the dense tail sheet, faster than in the perpendicular IMF-plane. The z-component of the velocity (along the tail direction) is shown in Fig. 1b and can be compared to the density distribution in Fig. 1a. In both planes, ions are faster, farther away from the tail axis.

The parameters used for the model are chosen to well describe the global large-scale comet - solar wind interaction. The $H_2O^+$ number density has been calculated using $H_2O^+$ ions as trace particles in the flow (see Rauer et al., 1995). Any chemical reaction other than photoionisation has been neglected. The rates for photoprocesses have been taken from Huebner et al. (1992). Elastic collisions of ions with neutrals do not influence the results discussed below, since collisional processes are important only close to the nucleus. Because the smallest model resolution around the nucleus is ≈8000 km, together with the fact that we are looking at large field of views when comparing with observations, this simplification is a valid assumption. However, ionization by solar wind particles may increase the number of ions. The contribution of chemistry to the effective ion flow will be subject of a subsequent publication.

## 3. Calculation of emission lines from the model

### *3.1. Procedure*

Every grid point of the model represents the local ion density, temperature and velocity. We assume that every such element along the LOS emits an emission line, G, which is described by a Gaussian. The Gaussian is determined by the following parameters: The width is given by the model ion temperature, $T_i$, and the position is determined by the velocity component along the LOS, $v_{LOS}$.

In the distant coma, $H_2O^+$ emission is mainly excited by fluorescence excitation. The lines are optically thin and therefore, the emission intensity depends only on the ion number density and the g-factor. We have not attempted to calculate the intensity directly from the model ion distribution, because the g-factors of observed emission lines are rather uncertain. Instead,

we simply scale the emitted Gaussian proportional to the $H_2O^+$ number density, n.

The Gaussian profile is given by:

$$G = n\sqrt{m_C/(2\pi k_B T_i)}exp(-\frac{m_c(v - v_{LOS})^2}{2k_B T_i}) \quad (1)$$

Here, $T_i$ is the ion temperature, $m_c$ the mass of a cometary particle as used in the model (20 amu), $v_{LOS}$ denotes the velocity component along the LOS, and $n$ corresponds to the ion number density.

In the case of optically thin emissions the resulting line profile, as observed from the ground, can be simply calculated by adding all emission lines along the LOS and inside a given field-of-view, FOV. The resulting line shape is determined by the temperature and velocity dispersion in the region of the plasma tail studied and the line intensity differs from the measured intensity only by a scaling factor.

### *3.2. Line shapes*

To illustrate how the shape of ion emission lines in cometary plasma tails is formed, an emission line has been calculated for the following observing geometry: the observer looks at an angle of 45° to a point 4 $10^5$ km behind the nucleus on the tail axis. Fig. 2a shows the individual Gaussian shaped lines emitted along the LOS. It is assumed that the tail is oriented such that the IMF plane faces the observer, and the LOS is along the equatorial plane. The displacement of the emission lines towards higher velocities farther from the tail axis can be seen. In Fig. 2b, the resulting added profile is shown (solid line). The ions with high velocity impose a strong asymmetry on the profile. For comparison, the same profile has also been calculated assuming that the equatorial plane is facing the observer (dashed line). The profiles for the orthogonal viewing directions differ substantially. Whereas a strong asymmetry is seen when viewing the IMF plane, the high velocity wing has almost disappeared when viewing the perpendicular tail side. In addition, the emission line intensity resulting from a view on the equatorial plane is reduced.

The different shape of emission lines is caused by the density and velocity distribution in the tail seen in Fig. 1a and b. When viewing the IMF (xz-) plane, the density distribution along the LOS falls off slowly. Therefore, the high velocity ions far from the axis are still abundant enough to contribute to the signal. In the perpendicular direction the density drops quickly, and emission from ions far from the tail axis is faint. The different density distribution along the LOS also causes the difference in intensity.

The orientation of the tail towards the observer depends on the interplanetary magnetic field, which is usually not known at the position of the comet during a measurement. However, the two orientations shown in Fig. 2 represent the two extreme cases. For any other tail configuration the resulting column density and line shape will be in between the two extremes shown.

Fig. 2c is similar to Fig. 2b, but now the FOV has been increased to a square of $10^5 \times 10^5$ km. The difference in intensity and line shape between the two tail orientations is reduced. A large FOV minimizes the influence of the tail orientation, as it approximates a more complete coverage of the total flow of cometary ions.

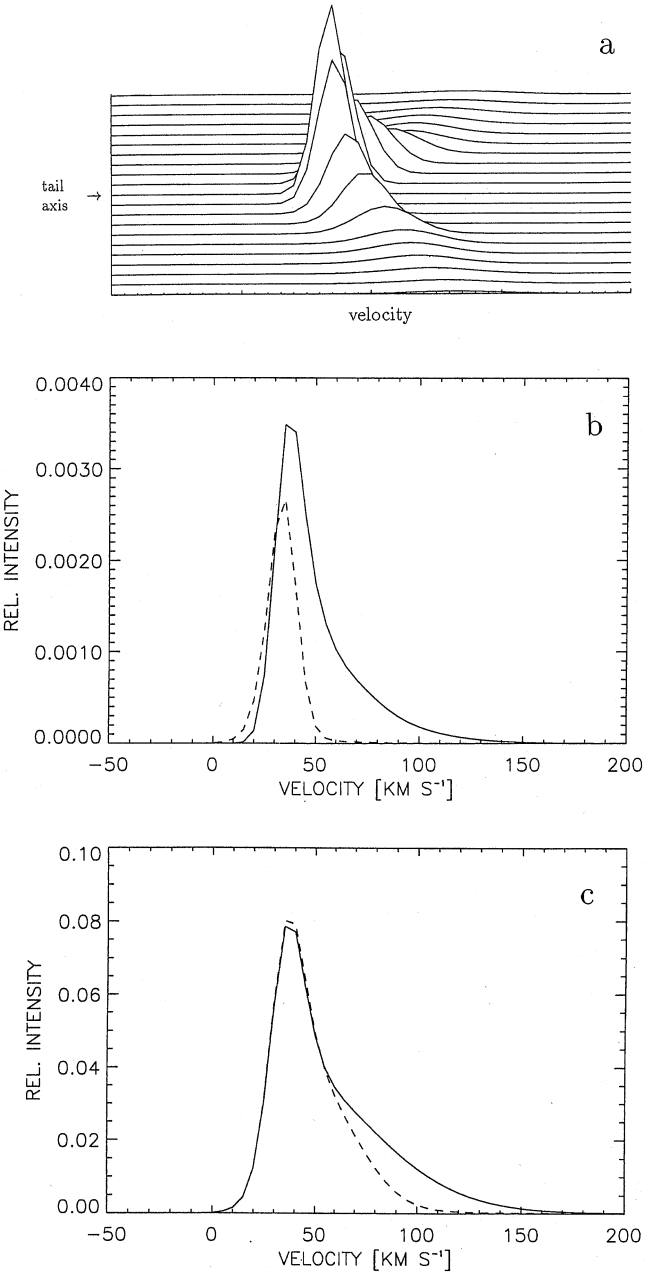


**Fig. 2a–c.** Line profile obtained from a 3D MHD model, looking under 45° at a point 4 $10^5$ km down the tail. **a** individual profiles along the LOS, looking at the IMF plane; **b** resulting added profile from the integration along one LOS, looking at the IMF plane (solid line) and looking at the equatorial plane (dashed line); **c** Same as in b, but increasing the FOV to $10^5$ km × $10^5$ km.

## 4. The data set

Spectra of the $H_2O^+$ doublet at 6159 Å have been taken in comet 1P/Halley in January 1986 (Scherb et al., 1990) with high signal/noise and spectral resolution. The spectra were obtained using the Wisconsin dual pressure scanned Fabry-Perot spectrometer at the McMath-Pierce solar telescope on Kitt Peak. The spectral resolution was 0.2 Å, which is not quite sufficient to resolve the two doublet lines at 6158.64 Å and 6158.85 Å, respectively. The size of the FOV was 3.5' in radius. The heliocentric distance, $r_h$, was 0.93 AU, the geocentric distance, $\Delta$, corresponded to 1.26 AU. The data set and analysis are described in detail in Scherb et al. (1990).

As the tail pointed away from the earth, the lines are progressively red shifted along the tail. In order to derive the antisolar velocity of the ions, Scherb et al. fitted the obtained lines with two gaussian shaped emission lines. The intensity ratio was assumed to be 3/2, according to the statistical weight of the spin doublet lines. Fig. 3 shows the scans of the $H_2O^+$ doublet (crosses) taken on January 6, 1986. The solid line corresponds to the two fitted Gaussians. Although the fit represents the data overall fairly well, deviations are clearly seen on the high-velocity side of the lines.

## 5. Comparison of data and model

### *5.1. Scaling of model to data*

With some simplifications the results obtained from a model of the comet-solar wind interaction for certain solar wind conditions and cometary gas production rates can be scaled to other parameters. In coordinates normalized to the size of the interaction region, $R_I$, all comets show identical flow patterns, as long as the spatial scales are small against the ionisation scale length (e.g.: Schmidt & Wegmann 1982; Wegmann 1995). Therefore, all spatial distances, $x$, can be normalized as

$$x_n = x/R_I; \qquad with \qquad R_I = \frac{\sigma m_C Q}{4\pi w \rho_\odot u_\odot}. \tag{2}$$

Here, $\sigma$ is the ionisation rate, $m_C$ the average neutral particle mass, $w$ the neutral particle velocity, Q gives the gas production rate and $\rho_\odot$ and $u_\odot$ correspond to the solar wind mass density and velocity, respectively. $R_I$ equals 8 $10^4$ km with the parameters of the model comet.

The scaling law offers the possibility of applying model results obtained for a certain cometary gas production rate and solar wind flux to various comets, without having to run a time consuming simulation for every comet and for every measurement along a comet's orbit.

When comparing the line shapes derived from the model with the $H_2O^+$ emission lines measured in comet 1P/Halley, appropriate scaling must be performed for both the distance of the aperture from the nucleus and the size of the FOV. Roughly speaking, for a comet with higher gas production rate the same conditions in the tail are found at larger distances from the nucleus compared to weaker comets. Due to the large gas production rate of comet 1P/Halley, larger spatial scales (like the bow shock distance) become comparable to the ionisation scale length, w/$\sigma$, so that linear scaling is not anymore applicable due to the exhaustion of neutrals. The scaling of water ions is also limited to regions of size 100000 km due to the dissociation time scale for neutral water of $10^5$ sec. However, when studying regions smaller than the bow shock distance the scaling performed here is still appropriate.

To compare with the model we have to calculate the size of the interaction region with the solar wind, $R_I$, in comet 1P/Halley at the time of the measurements. This requires knowledge of the ionisation rate, the cometary gas production rate and the solar wind parameters. Unfortunately, most of these parameters are not known with sufficient accuracy for the time the data were taken. Measurements of OH in comet 1P/Halley with IUE and in the radio give a water production rate of about 3-5 $10^{29}$ $s^{-1}$ (Feldman et al., 1987; Bockelee-Morvan et al., 1990; Schloerb et al., 1987) for the beginning of January 1986. However, the analysis of Hydrogen and [OI] observations give a value around 7-9 $10^{29}$ $s^{-1}$ (Smyth et al., 1993). Unfortunately, infrared observations of water, the most direct measurement, are not available for January 1986. The range of production rate values exceeds a factor of 2, introducing a large uncertainty into the calculation of the appropriate scaling parameter. In addition, nothing is known about the solar wind, except that it should be close to quiet solar wind conditions.

Because of the large uncertainties in the parameters needed to calculate the size of the interaction region for comet 1P/Halley, we have varied $R_I$ in a range of 2–7 $10^5$ km in steps of $10^5$ km. Emission lines have been calculated as outlined above for the given observing geometry. Because two doublet lines are overlapping in the data, two modeled emission lines are added with a fixed separation corresponding to the wavelength separation of the $H_2O^+$ doublet. The lines have an intensity ratio of 3/2. Then, the profile is convolved with the instrumental profile of the Wisconsin dual-etalon system. A multiplicative factor has been applied to fit the model line intensity to the measured line intensities. This procedure was carried out for every value of $R_I$. The best overall fit to the data from January 6, 1986, is obtained with $R_I^{Halley} = 3 \pm 1$ $10^5$ km.

We checked if the value for $R_I^{Halley}$ corresponding to the best fit is in agreement with comet 1P/Halley's gas production rate and typical solar wind values using Eq. (2). If we use a typical value for the quiet solar wind flux of 2.7 $10^8$ $cm^{-2}$ $s^{-1}$ (Schwenn 1990) to calculate the gas production from Eq. (2), we obtain a rate of 4.4 $\pm$1.4 $10^{29}$ $s^{-1}$ (the error corresponds solely to the uncertainty in $R_I$). The scaling parameter obtained for the best fit is therefore consistent with comet 1P/Halley's gas production, considering the large uncertainty in the solar wind conditions.

### *5.2. The Resulting comparison*

Fig. 4 shows again the data set displayed in Fig. 3. In addition, the profiles derived from the model for both viewing directions are presented. The line shapes fit the asymmetric wings of the

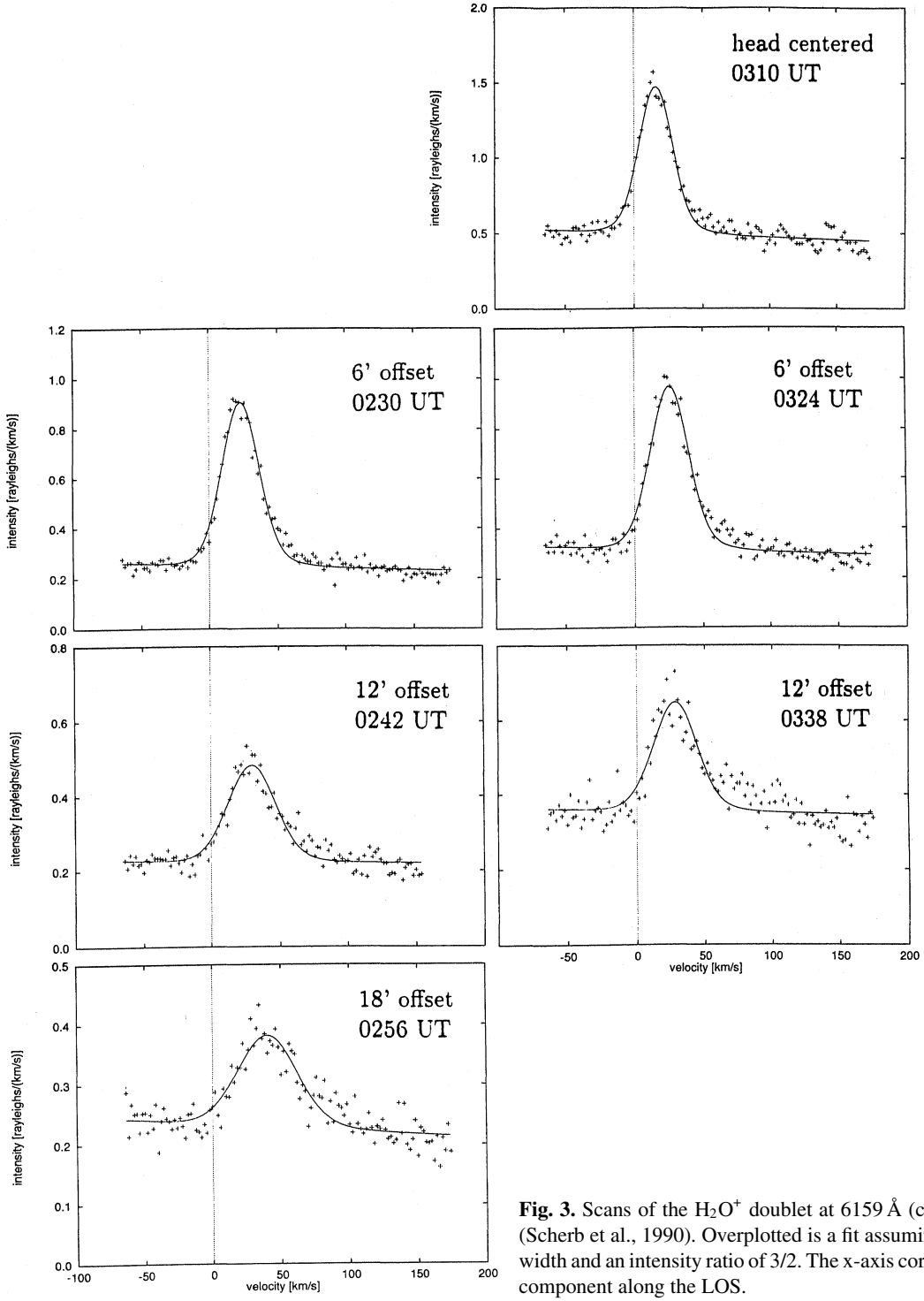


**Fig. 3.** Scans of the $H_2O^+$ doublet at 6159 Å (crosses) taken on January 6, 1986 (Scherb et al., 1990). Overplotted is a fit assuming two Gaussian profiles of equal width and an intensity ratio of 3/2. The x-axis corresponds to the measured velocity component along the LOS.

$H_2O^+$ lines well up to a distance of 12' from the nucleus. Further studies are required to investigate deviations at larger nucleocentric distances, where the measurements indicate even larger velocities than the model fit. Temporal variations in the solar wind might play a role. In general, the data are well reproduced by the model, showing that line-asymmetries caused by the velocity spread in the tail are indeed observed and are needed to fully approximate the measured spectra.

## 6. $H_2O^+$ production rates

All comets for which a water ion production rate could be determined show large discrepancies between the rates expected from photoionization and the measured values. Such difference is also found in the measurements of $H_2O^+$ in comet 1P/Halley on January 6, 1986. From the photoionization of water we expect about 3% (Huebner et al., 1992) of the water molecules

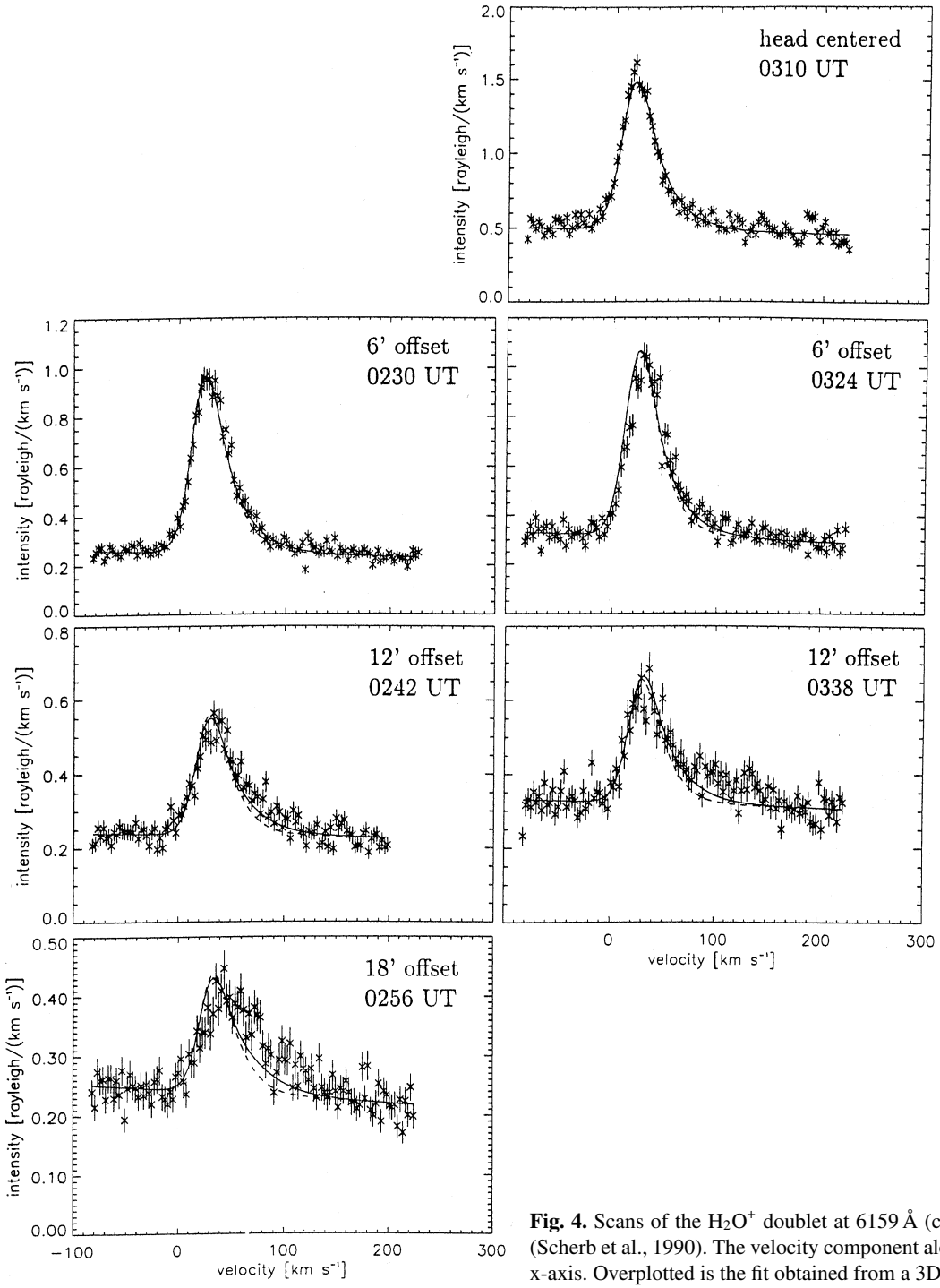


**Fig. 4.** Scans of the $H_2O^+$ doublet at 6159 Å (crosses) taken on January 6, 1986 (Scherb et al., 1990). The velocity component along the tail axis is given along the x-axis. Overplotted is the fit obtained from a 3D MHD model.

to be ionised, corresponding to a $H_2O^+$ production rate of 8-25 $10^{27}$ $s^{-1}$ for comet 1P/Halley on January 6, 1986.. The measured production rate (Schultz et al. 1993) is only $1.9\pm0.4$ $10^{27}$ $s^{-1}$. Thus, we have an order of magnitude discrepancy.

We have established that the model can reproduce the observed emission profiles. Now, we use it to evaluate the contribution of the different parts of the tail to the signal, and whether missed ions are sufficient to explain the discrepancy in flux measurements.

Several effects could be responsible for the reduced flow measured.

Ions are missed due to the limited size of the FOV. When observing from Earth, we always see all ions in the tail along the LOS (optically thin). However, due to the finite size of the FOV, ions far from the tail axis in the image plane, perpendicular to the LOS, are not seen in the measurement. Although the density of ions far from the axis is low, their velocity is high (compare Fig. 1), and they therefore might contribute significantly to the ion flux.

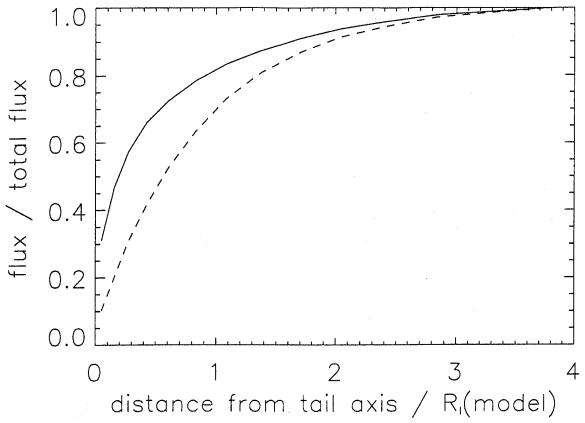


**Fig. 5.** Fraction of the flux in the ion tail to be measured in a slit perpendicular to the tail axis at $z_n$=5 behind the nucleus with increasing slit length. The x-axis corresponds to half the slit length in normalized coordinates. Orientation of the tail towards the observer: solid line: IMF plane; dashed line: equatorial plane.

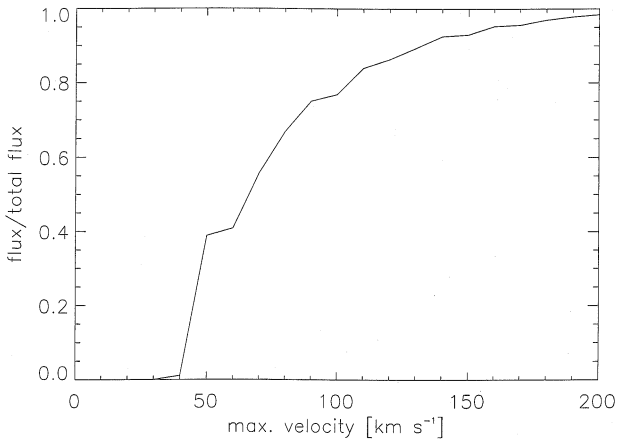


**Fig. 6.** Fraction of the flux in the ion tail up to a maximum ion velocity at $z_n$=5 behind the nucleus

To measure the ion flux it is best to concentrate on the part of the tail where the flow velocity is essentially parallel to the tail axis, that is in the tail at some distance from the nucleus, though smaller than the scale length for photo destruction of $H_2O^+$. If we assume that no ions are destroyed in the coma, the cometary ion production rate, Q, can be determined from the ion flux, F, through a cut in the tail by:

$$Q = F = \int nv_z dxdy \tag{3}$$

Here, $n$ is the ion number density, $v_z$ is their velocity component along the tail in the z-direction, and the integral is performed over the cut through the tail perpendicular to the tail axis.

To study the contribution of ions missed outside a given FOV, we have calculated the flux measured in a slit placed perpendicular to the tail axis in our model at a normalized distance $z_n$ = 5. Fig. 5 shows the ratio of the flux measured in the slit to the total ion flux as a function of the distance from the tail axis (the half slit length in normalized coordinates). The solid line corresponds to the IMF plane facing the observer, the dashed line to the perpendicular viewing direction. The measured flux increases with increasing slit length and approaches the total flux when the whole tail is in the slit. The difference of the two viewing directions results from the asymmetry of the ion distribution in the tail (see Fig. 1a and b). When performing the same study at a distance closer to the nucleus, where the ion distribution is more axisymmetric, the difference will be reduced. Farther down the tail, the difference between the orthogonal viewing directions increases with increasing flattening of the tail.

We can now use Fig. 5 to estimate the effect of the FOV on the measurements in comet 1P/Halley. The gas production rate measurements of 1P/Halley for January 1986 vary from 3-9 $10^{29}$ $s^{-1}$. With these rates we derive $R_I$ of 2.4 $10^5$ km and 7.2 $10^5$ km, respectively. Thus, with a FOV of 1.9 $10^5$ km we can read the flux to be measured in Fig. 5 at $x_n$ = FOV/$R_I$ to be 63% or 30% of the total flux, depending on the gas production rate. About 3% of the total water production is ionized to $H_2O^+$. Thus, for the lower gas production rate we expect a $H_2O^+$ flux of (3 $10^{29}$ $s^{-1}$ × 0.63 × 0.03) = 5.7 $10^{27}$ $s^{-1}$. Assuming the higher gas production rates to be correct, a $H_2O^+$ flux of 8.1 $10^{27}$ $s^{-1}$ would be expected. Thus, the limiting size of the FOV reduces the flux measured. However, a discrepancy of a factor of 3, or more, still remains.

Another explanation of the reduced ion flux measured is a significant amount of ions which might be redshifted by a large amount and fall outside the scanned range of velocities in the measurement (Schultz et al., 1993).

To investigate the contribution of fast ions in the tail to the ion flux, we determine again the flux at a distance of $z_n$ = 5 in the tail. However, now only ions up to a certain maximal velocity, $v_{max}$, are taken into account. Fig. 6 shows the ratio of this flux to the total flux as a function of the maximal velocity. We can see that ions faster than 200 km $s^{-1}$ contribute only less than 5% to the flux. Examining the line profiles in Fig. 4 shows that only at large offsets a significant contribution to velocities larger than 150 km $s^{-1}$ can be observed. Therefore, the contribution of fast ions which would fall outside the scanned velocity range cannot explain the low $H_2O^+$ flux measured.

Another possibility to explain the flux discrepancy are fast ions missed in the original data analysis because simple Gaussian profiles have been used to approximate the line profiles. As shown in the previous section, these fits were insufficient to approximate correctly the contribution of ions in the high-velocity wing of the lines. We take as example the line profile 12 arcmin offset from the nucleus in Fig. 3. Ions faster than about 70 km $s^{-1}$ are not approximated by the Gaussian profiles. We estimate the flux missed by calculating the flux in the model at the corresponding nucleus distance using only ions slower than 70 km $s^{-1}$ (similar to Fig. 6). About 70% of the flux should have been measured, even when using only a Gaussian profile to approximate the lines measured.

A third possibility to explain the low ion flux measured are enhanced losses of $H_2O^+$ ions in the inner coma by collisional reactions with $H_2O$ to form $H_3O^+$. However, in comet Halley $H_3O^+$ ions are important only within about $2\ 10^4$ km from the nucleus (Altwegg et al., 1993). This is small against the FOV of $1.9\ 10^5$ km in our observations. In addition, $H_3O^+$ ions are destroyed by dissociative recombination and again $H_2O$ is formed, which can subsequently be ionized. Therefore, the losses do not play a role in the observations of comet Halley. Additionally, new MHD models have been developed recently, which take into account in a selfconsistent way all important reactions of the water group ions and molecules. Preliminary results (Wegmann, private communication) show that ionization by charge exchange and electron impact by solar wind particles enhance the effective ionization so much that about 8% of the $H_2O$ molecules become ionized. The new model ion densities are appreciably higher than those of earlier models (Wegmann et al., 1987), but still too low compared to the densities measured by Giotto at comet 1P/Halley (Altwegg et al., 1993, Neugebauer et al., 1991). Thus, a more detailed modeling of the $H_2O^+$ chemistry will only increase the discrepancy between models and ground based observations.

Another possibility for the low $H_2O^+$ fluxes measured are uncertainties in the g-factors used to convert from intensities to column densities. The g-factors are calculated for whole emission bands only (Lutz 1987; DiSanti et al., 1990), and under the assumption of pure resonance fluorescence excitation. However, in most measurements only parts of a band or, as in the data discussed here, only a few lines are observed. To be able to convert to column densities, the band g-factor is usually divided by the relative strength of the observed emissions according to a calculation by Wyckoff & Wehinger (1976). This calculation is performed for a temperature of 100 K, thus assuming collisional excitation. However, collisional excitation is important only in the innermost coma, and the ion temperature is not constant. The relative line strength differs for different temperatures (see Wyckoff & Wehinger), and can also be different for fluorescent excitation, which is the dominant excitation mechanism throughout most of the tail. Uncertainties in the g-factor can therefore easily account for a factor of 2, or more, in the determination of column densities and ion fluxes. A detailed excitation model of $H_2O^+$ is strongly required.

## 7. Conclusions

The ion distribution given by a 3-D MHD model of the comet-solar wind interaction has been used to derive the profile of ion emission lines as measured in ground based spectra. The resulting lines are asymmetric, with a high-velocity wing caused by fast ions far from the tail axis. For a given FOV, the asymmetry depends on the orientation of the tail towards the observer. However, for large fields-of-view both viewing directions result in similar, asymmetric lines.

Line shapes derived from the model have been compared to spectra of an $H_2O^+$ doublet measured in comet 1P/Halley in January 1986. It could be shown that the line profile resulting from the model of the comet-solar wind interaction is able to approximate the measured line shape better than a fit of simple Gaussian profiles. This indicates that fast ions can indeed make a contribution to the measured signal and need to be taken into account when analysing measured line profiles.

The model of the cometary plasma tail has also been used to study quantitatively several possible causes for the discrepancy between measured and expected $H_2O^+$ production rates in comets. It could be shown that neither the limited size of the FOV, nor fast ions which are outside the scanned range or in the high-velocity wing of the line profile, can explain the whole discrepancy between the measured flux and the flux expected from photoionization of water. Uncertainties in the g-factors seem to be the most likely explanation of the remaining difference. However, this has to be validated by an improved model of the $H_2O^+$ excitation.

Observations of future comets (like comet Hale-Bopp) with improved measurements of the water and water ion production rates will allow a more stringent quantitative comparison of measured and expected rates with the aid of a comet-solar wind interaction model.

*Acknowledgements.* We thank Kurt Retherford who helped making the data on comet 1P/Halley available to us. We also thank J. Crovisier and W.-H. Ip for interesting discussions. H. Rauer acknowledges the support of an ESA external research fellowship.

## References

Altwegg, K., Balsiger, H., Geiss, J., et al., 1993, A&A 279, 260
Bockelée-Morvan, D., Crovisier J., Gérard E., 1990, A&A 238, 382
DiSanti, M.A., Fink U., Schultz, A.B., 1990, Icarus 86, 152
Feldman, P.D., Festou, M.C., A'Hearn, M.F., et al., 1987, A&A 187, 325
Huebner, W.F., Keady, J.J., Lyon S.P., 1992, Astrophys. Space Sci. 195, 1
Lutz, B., 1987, ApJ 315, L147
Neugebauer, M., Goldstein, R., Goldstein, B.E., et al., 1991, ApJ 372, 291
Rauer H., Jockers, K., 1993, Icarus 102, 117
Rauer H., Wegmann, R., Schmidt, H.U., Jockers, K., 1995, A&A 295, 529
Scherb, F., Magee-Sauer, K., Roesler, F.L., Harlander, J., 1990, Icarus 86, 172
Schloerb, F.P., Claussen M.J., Tacconi-Garman, L., 1987, A&A 187, 469
Schmidt, H.U., Wegmann, R., in: Wilkening, L. (ed.) 1982, Comets, University of Arizona Press, Tucson, AZ, 538.
Schmidt-Voigt, M., 1989, A&A 210, 433
Smyth, W.H., Marconi, M.L., Scherb, F., Roesler, F.L., 1993, ApJ 413, 756
Schultz, D., Scherb, F., Roesler, F.L., 1993, Icarus 104, 185
Schwenn, R., 1990, in: Physics and Chemistry in Space - Space and Solar Physics, Vol.20, Physics of the Inner Heliosphere I, R. Schwenn, E. Marsch (eds.), Springer Verlag, 99
Wegmann, R., Schmidt, H.U., Huebner, W.F., Boice, D.C., 1987, A&A 187, 339
Wegmann, R., 1995, A&A 294, 601
Wyckoff, S., Wehinger, P.A., 1976, ApJ 204, 616